

Biochemistry. Author manuscript; available in PMC 2014 August 27.

Published in final edited form as:

Biochemistry. 2013 August 27; 52(34): . doi:10.1021/bi4008935.

Na+/substrate Coupling in the Multidrug Antiporter NorM Probed with a Spin-labeled Substrate

P. Ryan Steed, Richard A. Stein, Smriti Mishra, Michael C. Goodman, and Hassane S. Mchaourab *

Department of Molecular Physiology and Biophysics, Vanderbilt University, Nashville, TN 37232

Abstract

NorM of the multidrug and toxic compound extrusion (MATE) family of transporters couples the efflux of a broad range of hydrophobic molecules to an inward Na⁺ gradient across the cell membrane. Several crystal structures of MATE transporters revealed distinct substrate binding sites leading to differing models of the mechanism of ion-coupled substrate extrusion. In the experiments reported here, we observed that a spin-labeled derivative of daunorubicin, Ruboxyl, is transported by NorM from *Vibrio cholerae*. It is therefore ideal to characterize mechanistically relevant binding interactions with NorM and to directly address the coupling of ion and drug binding. Fluorescence and EPR experiments revealed that Ruboxyl binds to NorM with micromolar affinity and becomes immobilized upon binding, even in the presence of Na⁺. Using double electron-electron resonance (DEER) spectroscopy, we determined that Ruboxyl binds to a single site on the periplasmic side of the protein. The presence of Na⁺ did not translocate the substrate to a second site as previously proposed. These experiments surprisingly show that Na⁺ does not affect the affinity or location of the substrate binding site on detergent-solubilized NorM, thus suggesting that additional factors beyond simple mutual exclusivity of binding, such as the presence of a Na⁺ gradient across the native membrane, govern Na⁺/drug coupling during antiport.

Resistance of bacteria to antibiotics is a significant obstacle to the clinical treatment of infections. One key mechanism of resistance is the active efflux of cytotoxic molecules across the cell membrane, executed by functionally diverse families of transporters with overlapping substrate specificities. The multidrug and toxic compound extrusion (MATE) family encompasses ion/drug antiporters occurring in diverse organisms from bacteria to humans with 12-13 transmembrane (TM) helices in a topology distinct from transporters of the major facilitator superfamily. ^{2,3} Several known MATE transporters, including NorM from Vibrio cholerae (Vc), couple the efflux of a broad range of compounds to an inward Na⁺ gradient.^{2,4,5} Biochemical studies of NorM from *Vibrio parahaemolyticus* (77% identical to Vc-NorM) identified several conserved, membrane-embedded acidic residues involved in Na⁺-coupled transport. He et al. reported a structure of Na⁺-coupled Vc-NorM in an open-outward state. No substrate was resolved in this moderate resolution structure, but observation of bound Rb⁺ and Cs⁺ ions suggested a location of the ion binding site in proximity to the conserved acidic residues Glu255 on TM7 and Asp371 on TM10. A molecular dynamics simulation of Na⁺ binding to Vc-NorM supported this binding location and also predicted transient binding of Na⁺ at conserved Asp36 on TM1.⁸

^{*}Correspondence to: Hassane Mchaourab, Department of Molecular Physiology and Biophysics, 741 Light Hall, 2215 Garland Ave., Nashville, TN, 37232, USA; Tel.: (615) 322-3307; hassane.mchaourab@vanderbilt.edu.

Supporting Information—An additional introductory figure, raw DEER decays, and details of DEER data analysis are available free of charge via the internet at http://pubs.acs.org.

Two sets of crystal structures of MATE transporters have begun to address the location(s) of drug binding (Fig. S1). One set of structures of Na⁺-coupled NorM from *Neisseria gonorrhea* (*Ng*; 34% identical to *Vc*-NorM) identified ethidium, rhodamine 6G, or tetraphenylphosphonium (TPP) bound to the periplasmic side of the open-outward state (*i.e.* open to the periplasm) in a site distinct from the Na⁺ binding site. Additionally, Tanaka *et al.* reported structures of a H⁺-coupled MATE transporter from *Pyrococcus furiosus* (*Pf*) that revealed norfloxacin bound in a cavity in the middle of the membrane. A pH-dependent obstruction of this cavity, resulting from protonation of conserved Asp41 (Asp36 in *Vc*-NorM), suggested a mechanism of substrate dissociation. The prediction that Na⁺ also interacts with this Asp raises the possibility that the same mechanism may operate in Na⁺-coupled MATE transporters and that the distinct substrate binding sites observed in *Ng*-NorM and *Pf*-MATE represent ion-dependent steps in drug extrusion.

Fluorescent substrates have long been used to probe substrate binding sites and provide mechanistic insight, ¹¹ but their utility is often limited by various sources of interference, particularly for multidrug transporters where substrates tend to be hydrophobic and therefore partition into bilayers. This partitioning confounds interpretation of changes in substrate fluorescence as both lipid and transporter binding lead to increased fluorescence. Alternatively, electron paramagnetic resonance (EPR) spectroscopy with spin-labeled substrates is virtually free from interference and can reveal the environment of the label, its accessibility, and its distance from other spin labels. For example, Omote and al-Shawi¹² used spin-labeled verapamil to measure binding to human P-glycoprotein and active uptake of this substrate into proteoliposomes. More recently, Gaffney *et al.*¹³ mapped the binding site of a spin-labeled lipid in soybean lipoxygenase-1.

In this study, we use a spin-labeled derivative of daunorubicin, Ruboxyl, to probe the substrate binding site on Na⁺-coupled Vc-NorM and its response to Na⁺. This compound was developed previously to reduce oxidative side effects of chemotherapeutic daunorubicin treatment. It contains a fluorescent anthracycline moiety and a tetramethylpiperidone nitroxide attached via a hydrazone linker (Fig. 1). We show that NorM has a micromolar affinity for Ruboxyl even in the presence of Na⁺, and that Ruboxyl binds at a site where the motion of the spin label moiety is restricted yielding an immobilized lineshape consistent with high-affinity binding. We used double electron-electron resonance (DEER) spectroscopy 15–17 to locate the high-affinity binding site on NorM in the apo and Na⁺-bound states. These experiments show that substrate binds at a single site on Vc-NorM and that Na⁺ does not induce substrate translocation to a second, distinct site. Furthermore, we establish Ruboxyl as a useful probe for drug binding in order to address questions of the mechanism of ion-coupled antiport of hydrophobic molecules.

EXPERIMENTAL PROCEDURES

Test substrates

Ruboxyl was obtained from Ambinter, Orléans, France. For binding experiments, concentrations of stock solutions of test substrates were determined spectrally as follows: Ruboxyl, daunorubicin, doxorubicin, A_{480} in H_2O , = 11,500 M^{-1} cm⁻¹; rhodamine 6G, A_{530} in ethanol, = 116,000 M^{-1} cm⁻¹. Stocks of test substrates were diluted with GF buffer (50 mM HEPES/MES-NaOH, 0.05% - DDM, pH 7.5).

Drug resistance assay

Drug sensitive *Escherichia coli* BL21 7 (denoting the deletion of seven genes associated with multidrug resistance: *macAB*, *yojHI*, *acrAB*, *acrEF*, *emrAB*, *emrKY*, and *mdtEF*) cells¹⁸ were freshly transformed with empty pET19b or pET19b encoding wild-type or

mutant NorM with an N-terminal 10-His tag under the control of the inducible T7 promoter. A dense overnight culture of the transformant was used to inoculate 5 ml LB broth containing 0.1 mg/ml ampicillin and 0.1 mM IPTG. Aliqouts (10 µl) of cells in the exponential growth phase (A_{600} =1.0) were used to inoculate wells of a microplate containing 50% LB broth, 0.1 mg/ml ampicillin, 10 µM IPTG, and 0-34 µM Ruboxyl or doxorubicin. Cell density was measured by A_{600} on a microplate reader after 5 h growth at 37 °C and shaking at 200 rpm. Density was normalized to the density of the wells containing the lowest drug concentration.

Site-directed mutagenesis

WT *norM* in pET19b was used as the template plasmid for construction of Cys-less NorM, which in turn was used as the template for generation of single Cys substitutions. Substitution mutations were generated using a single-step PCR in which the entire template plasmid was replicated from a single mutagenic primer. Template plasmid was subsequently degraded by *DpnI* digestion. Plasmids were propagated using XL-1 Blue or DH5 cells and mutations were confirmed by DNA sequencing.

Expression and purification of NorM

BL21 (DE3) cells were freshly transformed with a pET19b vector encoding WT or mutant NorM with an N-terminal 10-His tag. A transformant colony was used to inoculate a 20 ml LB culture and subsequently 1 L of minimal medium A as previously described. 19 Cultures were incubated with shaking at 37 °C until reaching an OD₆₀₀ of 1.0 at which time the expression of NorM was induced by the addition of IPTG to 1 mM. The cultures were incubated an additional 4 h at 30 °C and then harvested and stored overnight at -20 °C. Cell pellets were resuspended in 20 ml lysis buffer (20 mM Tris-HCl, 20 mM NaCl, 30 mM imidazole, 5% (v/v) glycerol, pH 8.0) including 10 mM DTT and lysed by four passes through an Avestin C3 homogenizer. Cell debris was removed by centrifugation at $9000 \times g$ for 10 min. Membranes were collected from the supernatant by centrifugation at $200,000 \times g$ for 1 h. Membrane pellets were resuspended in lysis buffer containing 1% dodecylmaltoside (-DDM) and 0.5 mM DTT and incubated on ice with stirring for 30-45 min. Insoluble material was cleared by centrifugation at $193,000 \times g$ for 30 min. Cleared extract was loaded onto a 4 ml Ni-NTA affinity column equilibrated in Ni buffer (20 mM Tris-HCl, 20 mM NaCl, 0.05% w/v -DDM, pH 8.0) at a flow rate of 1.5 ml/min. After washing with 5 column volumes of Ni buffer containing 30 mM imidazole, NorM was eluted with Ni Buffer containing 300 mM imidazole. Eluate was concentrated to 0.5 ml with a spin concentrator (100 kDa, Millipore) and injected onto a Superdex 200 column (GE) equilibrated with GF buffer with or without 20 mM NaCl. Purified NorM was concentrated using a spin concentrator (100 kDa), and the final concentration was determined by A₂₈₀ ($= 1.075 \text{ mg}^{-1} \text{ cm}^{-1}$). Purified NorM was stored on ice until use within one week.

Fluorescence anisotropy

Dilutions of WT or Cys-less NorM in GF buffer were mixed with a constant concentration of a test substrate in a total volume of 25 μ l in a 384-well black microplate and incubated at room temperature >5 min. Anisotropy of daunorubicin, doxorubicin, and Ruboxyl fluorescence ($_{ex}$, 485 nm; $_{em}$, 595 nm) was measured using a BioTek Synergy H4 microplate reader.

CW-EPR spectroscopy

Dilutions of Cys-less or Cys-substituted, spin-labeled NorM in GF buffer with or without 20 mM NaCl were mixed with a constant concentration of a test substrate in a total volume of

 $25 \mu l$ and transferred to a glass capillary. Spectra were collected on a Bruker EMX spectrometer with microwave power of $10 \mu l$ mW and modulation amplitude of $1.6 \mu l$ G.

Binding analysis

Fluorescence anisotropy values and the heights of the high field resonance lines from CW-EPR spectra were fit with a binding model assuming one site on NorM (P) where affinity for Ruboxyl (L) is described by a dissociation constant, K_D ($K_D = [P][L]/[PL]$). In this system, Ruboxyl binds to NorM, partitions into DDM micelles, and non-specifically associates with the NorM:DDM complex. Since it is not practical to deconvolute these binding events, we use [PL] here to describe all Ruboxyl not free in solution. Therefore, K_D values describe an amalgamation of all binding events present in the system. Depletion of unbound NorM and Ruboxyl was accounted for by subtracting NorM and Ruboxyl present in complex (PL) from the total starting concentrations ([P] = P_{total} – [PL]; [L] = L_{total} – [PL]). Combination of these equations results in a quadratic, which was used to fit the data in Origin 8 (OriginLab Corp., Northampton, MA). The contributions of signal from bound (I_{bound}) and unbound $(I_{unbound})$ Ruboxyl molecules was related to the total signal (I_{total}) by the equation, I_{total} $f_{\text{bound}}I_{\text{bound}} + f_{\text{unbound}}I_{\text{unbound}}$, where f_{bound} and f_{unbound} are the fractions of bound (from $[PL]) \ and \ unbound \ (from \ [L]) \ Ruboxyl, \ respectively. \ I_{unbound} \ is \ the \ fluorescence \ anisotropy$ value or height of the high field line of Ruboxyl with no NorM present. Ibound is the yasymptote of the binding data, dependent on the fit, and is an amalgamation of signal from all bound species. The K_D from the resulting curve represents an apparent K_D of detergentsolubilized NorM, which includes contributions from the partitioning of Ruboxyl into detergent micelles and non-specific association (see Results).

DEER spectroscopy

Dilutions of Cys-less or Cys-substituted, spin-labeled NorM in GF buffer were mixed with the indicated concentrations of test substrates and/or NaCl in a total volume of 10 μ l. Glycerol was added to samples to a final concentration of 30% (w/v) as a cryoprotectant. Dipolar time evolution data was collected at 83 K on a Bruker Elexsys E580 spectrometer operating at Q-band frequency (34 GHz) using a standard four-pulse protocol. ²⁰ Raw spin echo decays were analyzed using DeerAnalysis 2011 and fit using Tikhonov regularization or a single Gaussian model (Fig. S2).

Water accessibility measurement

Cys-less NorM and Ruboxyl were mixed in a 4:1 ratio and then passed through a spin concentrator (100 kDa) to deplete unbound Ruboxyl. Power saturation curves were measured in a gas-permeable TPX capillary equilibrated in N_2 as previously described. Final concentration of Ni-EDDA was 50 mM.

RESULTS

NorM transports Ruboxyl

To determine whether Ruboxyl is suitable to probe substrate binding throughout the transport cycle, we tested Ruboxyl transport by Vc-NorM using an $in\ vivo$ drug resistance assay. Drug-sensitive $E.\ coli\ BL21$ 7 cells 18 expressing WT Vc-NorM or harboring the empty vector were cultured in the presence of various concentrations of Ruboxyl or doxorubicin, a known substrate of Vc-NorM. 5,7 Ruboxyl was toxic to cell growth with an IC $_{50}$ of $\sim 3\ \mu\text{M}$ compared to an IC $_{50}$ of $\sim 1\ \mu\text{M}$ for doxorubicin. Expression of Vc-NorM, induced by a low concentration of IPTG, enabled cell growth at higher concentrations of Ruboxyl and doxorubicin relative to growth of the non-expressing cells (Fig. 2A). These results suggest that NorM actively extrudes Ruboxyl from the cytoplasm.

Ruboxyl binds to WT and Cys-less NorM with micromolar affinity

To facilitate experiments with Cys-substituted NorM we used site-directed mutagenesis to generate a NorM construct in which the three endogenous Cys residues at positions 196, 330, and 369 were mutated to Ala, Thr, and Val, respectively. Function of Cys-less NorM was confirmed by measuring resistance to doxorubicin in the above drug resistance assay (Fig. 2A). We determined the binding affinity of detergent-solubilized Cys-less NorM for Ruboxyl by taking advantage of the fluorescence of the anthracycline moiety ($_{\rm ex}$, 485 nm; $_{\rm em}$, 595 nm). We measured the fluorescence anisotropy of 0.2 μ M Ruboxyl at concentrations of NorM from 0.01 to 100 μ M. The binding curve was fit with a classic binding model assuming a single binding site characterized by a dissociation constant, K_D . The fit yielded an apparent K_D of 1 μ M (Fig. 2B). We use "apparent" here because measurement of the intrinsic K_D was hindered by partitioning of Ruboxyl into $\,$ -DDM micelles, which appears to be enhanced by non-specific interactions with NorM in these micelles (see below). Binding affinities of Cys-less NorM for doxorubicin and Ruboxyl were identical to wild type (Fig. 2B and Table 1). Therefore, subsequent experiments were carried out with the Cys-less construct.

Ruboxyl becomes immobilized upon binding

Ruboxyl offers the added benefit of detection of binding by the immobilization of the spin label moiety, evident by changes in the CW-EPR spectral lineshape. In GF buffer with 20 mM Na⁺ and detergent but no NorM, the EPR lineshape of Ruboxyl was characteristic of fast motion, as expected for free tumbling in solution (Fig. 3A, black). Incubation of Ruboxyl with NorM resulted in a multi-component spectrum (Fig. 3A, red). The most mobile component, characterized by sharp resonance lines, is similar to that observed in buffer without NorM and arises from the fraction of Ruboxyl that remained unbound in solution. The least mobile component, characterized by the outer extrema (inset in Fig. 3A), is consistent with loss of isotropic motion and arises from Ruboxyl bound to NorM in a sterically restrictive environment. To quantitate binding, we measured the height of the high-field resonance line (star in Fig. 3A) at increasing concentrations of NorM. The intensity of this line has little contribution from the spectrum of bound Ruboxyl, which is significantly broader. Therefore, this line best represents the fraction of unbound Ruboxyl. The binding curve, determined from the decrease in peak height of the high field resonance line (Fig. 3B), and calculated as described in "Experimental Procedures," indicated an apparent K_D of 1.5 μ M, consistent with the value determined by fluorescence anisotropy. We observed a similar binding curve for wild type NorM (data not shown).

Even at saturating concentrations of NorM (11-fold molar excess over Ruboxyl), a small fraction of the fast, free signal remained in the CW-EPR spectrum (~12% from the experiment in Figure 3, A and B). This signal could arise from free spin label hydrolyzed from Ruboxyl or a fraction of Ruboxyl that partitions into detergent micelles and is not accessible to NorM. We repeated several points of the binding curve using five-fold higher concentrations of Ruboxyl and NorM while holding the -DDM concentration constant. In this experiment (Fig. 3C), the fraction of spins remaining in the fast component in the presence of excess NorM was reduced to approximately 1.5%, suggesting that these spins remain mobile due to the partitioning of Ruboxyl molecules into -DDM micelles rather than hydrolysis of the label. The concentration of spins contributing to the fast component of the spectrum (1-2 μ M) was on the order of the concentration of empty -DDM micelles (0.05% (w/v) -DDM = 7.0-8.8 μ M). This calculation assumes an aggregation number of 110-140,²⁴ though Anatrace® reports values from 78-149.

NorM substrates, but not Na+, displace Ruboxyl at the high-affinity site

To determine whether Ruboxyl binds to a site shared by other known substrates, we added NorM to a mixture of Ruboxyl and an excess of doxorubicin, daunorubicin, or rhodamine 6G to compete for the Ruboxyl binding site in the presence of 20 mM NaCl. Ruboxyl binding was gauged by the height of the high field resonance line. Figure 4A shows that approximately half of the Ruboxyl molecules bound NorM even in the presence of 50-fold excess competitor. The CW-EPR lineshape of Ruboxyl in the presence of NorM and excess doxorubicin (Fig. 4B) showed a reduction of the immobilized component, indicating that competitors block Ruboxyl binding to the high affinity site. This competition suggested that approximately half of Ruboxyl molecules bind to the drug binding site shared with known substrates, but that additional Ruboxyl molecules bind elsewhere on NorM (see below). We observed a similar degree of competition in the absence of Na⁺ (data not shown).

Because NorM is a Na⁺-coupled transporter, we measured the effect of Na⁺ on Ruboxyl binding using the EPR lineshape by preparing Cys-less NorM in Na⁺-free buffer. Ruboxyl binding, as measured by the height of the high field resonance line, was nearly identical to binding in the presence of 20 mM Na⁺ and indicated an apparent K_D of 1.8 μ M (Fig. 3B). Furthermore, inclusion of Na⁺ in a mixture of Ruboxyl and NorM did not prevent Ruboxyl binding (Fig. 4C).

Additional Ruboxyl molecules bind non-specifically

The inability of competitors to completely prevent Ruboxyl binding suggested that Ruboxyl molecules may also bind NorM non-specifically. The lineshape of the population of Ruboxyl molecules that binds to NorM in the presence of doxorubicin was more restricted than free Ruboxyl but more mobile than bound Ruboxyl, consistent with lower affinity binding or non-specific association (Fig. 4B). We hypothesize that this component results from the partitioning of Ruboxyl molecules into detergent micelles containing NorM, possibly interacting with its surface.

Non-specific binding of Ruboxyl to detergent and/or NorM could interfere with experiments to localize the substrate binding site. Therefore, we determined conditions to select for Ruboxyl binding in the specific, competitor-sensitive site. When more than one Ruboxyl molecule is bound to the NorM:DDM complex simultaneously, it should be possible to detect a dipolar interaction between the two nitroxide moieties. The CW-EPR spectra collected during the experiments shown in Figures 3 and 4 did not indicate short range dipolar coupling suggesting that the binding sites must place the multiple spin-label moieties >20 Å apart. Therefore, we used DEER spectroscopy to detect a longer range dipolar interaction. With a six-fold molar excess of NorM, only the primary, high affinity binding site on NorM should be occupied by Ruboxyl. At the other end of the range, a three-fold excess of Ruboxyl should occupy every available site on NorM and in complex with detergent. Consistent with this model, the relative depth of modulation of the echo decay, which is an indicator of the fraction of interacting spins at a constant total concentration of Ruboxyl, increased with decreasing amounts of NorM (Fig. 5A). This result demonstrates that excess Ruboxyl promoted binding to non-specific sites in the NorM:micelle complex. The depth of modulation appeared to approach a maximum with three-fold excess of Ruboxyl suggesting that 2-3 Ruboxyl molecules bind on the NorM:DDM complex. No echo decay was observed with Ruboxyl in DDM micelles when NorM was absent (data not shown) indicating that one of the sites is specific to NorM: presumably the high-affinity site characterized by the immobilized lineshape. The shapes of the spin echo decays at each NorM:Ruboxyl ratio were consistent with broad distributions of distances from 20-60 Å reflecting the high degree of disorder in at least one of the binding sites. To confirm that the dipolar interaction involved the Ruboxyl molecules occupying the high affinity site, we

measured the echo decay of 1.4:1 NorM:Ruboxyl in the presence of excess doxorubicin. The competitor reduced the dipolar interaction to almost undetectable levels (Fig. 5B), which we interpret as the competitor excluding Ruboxyl from the high-affinity site.

High-affinity Ruboxyl binding occurs at a single site

Because Ruboxyl bound at the high-affinity site is highly ordered, as evidenced by the immobilized spectral lineshape, it was possible to measure distances between bound Ruboxyl and single spin-labeled sites on NorM. For this purpose, we introduced single spin labels at positions 44, 54, 125, 267, 269, and 338 on the periplasmic side of Vc-NorM and at position 216 on the cytoplasmic side (Fig. 6A). These positions were selected based on their locations at the ends of helices surrounding the putative drug binding cleft. We measured the distances between each site and bound Ruboxyl in the absence of Na⁺ using DEER spectroscopy. Experiments were carried out with a four-fold excess of NorM to select for Ruboxyl binding to the high affinity site and to reduce non-specific binding. For Ruboxylbound NorM labeled at positions 125, 216, 267, 269, and 338, we observed oscillating spin echo decays (Fig. S2) indicative of well-defined distributions of distances centered at 25 Å, 42 Å, 17 Å, 23 Å, and 34 Å, respectively (Fig. 6B). The narrow distance distributions are consistent with Ruboxyl binding at a single, specific site. We confirmed that the dipolar interaction between Ruboxyl and the label at position 216 arose from Ruboxyl bound in the high-affinity site by measuring the spin echo decay in the presence of excess doxorubicin. The presence of competitor greatly attenuated the oscillation in the spin echo decay by excluding Ruboxyl from the high-affinity site (Fig. S3). Additionally, we observed dipolar coupling in the CW-EPR spectra of Ruboxyl-bound NorM labeled at positions 44 and 54 indicated by broadening of the low-field resonance line (Fig. 6C).

Location of the Ruboxyl binding site

Distance distributions from DEER experiments were used to locate the position of the nitroxide moiety of Ruboxyl bound to NorM using the crystal structures of NorM as a scaffold. To facilitate this triangulation, we first modeled the spin label rotamers at the seven labeled sites on structural models derived from the crystal structures of cation-bound Vc-NorM (PDB: 3MKT) and rhodamine-bound Ng-NorM (PDB: 4HUN) using the program MMM.²⁵ This program generates rotamers of the spin label side chain that are sterically compatible with the modeled protein structure at the labeled site. A potential position of the Ruboxyl nitroxide was triangulated using distances from the top 26 rotamers for spin labels at positions 125, 216, 267, 269, and 338. To accommodate potential errors in the structural model and rotamer placement, we carried out fitting with all combinations of three distances (to reduce the weight of any one spin label position in the fitted position of Ruboxyl), and allowed the position of the Ruboxyl nitroxide to deviate from the measured DEER distance by ~4 Å. This fitting procedure yielded up to 17,576 potential positions from each of the ten sets of spin label combinations. To cull the number of potential positions, we eliminated those positions incompatible with short range dipolar coupling interactions with spin labels at positions 44 and 54 (i.e. 10-27 Å from the C position of these residues). To further restrict the placement of potential Ruboxyl positions, we determined the exposure of the Ruboxyl nitroxide to water by measuring the frequency of collisions with Ni-EDDA, a water-soluble paramagnetic relaxing agent. Low to moderate accessibility to Ni-EDDA (=0.45) allowed us to restrict potential positions to those inside the binding cleft, which is also consistent with the immobilized EPR lineshape.

This constrained triangulation procedure using the structure of *Vc*-NorM (PDB ID: 3MKT) generated a band of potential Ruboxyl nitroxide positions on the periplasmic side of the open cleft running from TM 3 along the C-terminal half of the cleft and ending at TM 8 (Fig. 7A). Notably, there is a confluence of points between TMs 2 and 7 consistent with all

combinations of distances (arrow in Fig. 7A). Because this method depends on the reliability of the backbone assignments in the crystal structure, we also carried out the triangulation procedure using the higher-resolution, substrate-bound structure of Ng-NorM (PDB ID: 4HUN). Equivalent amino acid positions between Vc-NorM and Ng-NorM were derived from the alignment reported by Lu et al. Significantly, this alignment places residue 125 in the loop between TMs 3 and 4 rather than on TM 4, thus displacing the position of the carbon by 15 Å (compare Fig. 7, B and C). For this reason, we used a set of sixteen combinations of three distances, which included distances from either the end of TM 4, consistent with the structural position of 125 in Vc-NorM (137 in Ng-NorM), or the 3-4 loop, the equivalent position in Ng-NorM (131) based on the sequence alignment. A similar band of potential Ruboxyl nitroxide positions in the periplasmic cleft was generated. Measurement from the 3-4 loop position of 125 places the Ruboxyl nitroxide in the cleft near the periplasmic end of TM 8 (Fig. 7B), but this location is not consistent with all distances. When the distance is measured from the TM 4 position of 125, a confluence of points appeared between TMs 2 and 7 similar to the cluster generated on the Vc-NorM scaffold (arrow in Fig. 7C). This cluster of potential positions of the Ruboxyl nitroxide is consistent with the placement of the high-affinity Ruboxyl binding site in the periplasmic cleft.

Na+ does not alter the location of Ruboxyl binding

To address the possibility that Na⁺ binding drives substrate translocation to a distinct binding site, we measured the distances from Ruboxyl to the above spin labeled sites in the presence of 70 mM NaCl. For Ruboxyl-bound NorM labeled at positions 125, 216, 267, 269, and 338, we observed oscillating spin echo decays resulting in distance distributions similar to those observed in Na⁺-free conditions (Fig. 8A). For Ruboxyl-bound NorM labeled at positions 44 and 54, broadening of the CW-EPR lineshape due to dipolar coupling was similar to broadening observed in Na⁺-free conditions (Fig. 8B). These results indicate that the position of the nitroxide of Ruboxyl is not altered by the presence of Na⁺.

DISCUSSION

Current models of antiport by MATE family transporters based on the crystal structures of Vc-NorM, $^7Ng\text{-NorM}$, and $Pf\text{-MATE}^{10}$ propose a conformational change, induced by binding of the coupling ion, that results in reduced binding affinity for substrates (Fig. S1). Additionally, the substrate binding site observed in Ng-NorM differs from that observed in Pf-MATE raising the possibility of ion-driven translocation of substrate through multiple sites during transport. In this study, we have identified a spin-labeled substrate of Vc-NorM, Ruboxyl, and used EPR spectroscopy to monitor this substrate in its binding site in order to address questions of drug binding and translocation during ion-coupled antiport by a MATE transporter. We found that Ruboxyl binds to a single, periplasmic site and that neither the affinity nor the location of this site are altered by Na⁺. Independence of substrate and Na⁺ binding conflicts with the classical model of antiport in which binding of substrate and coupling ion are mutually exclusive and thus raises questions about the mechanism of coupling in NorM during drug antiport.

Ruboxyl is a spin-labeled derivative of daunorubicin, a known substrate of NorM.⁵ We show that Ruboxyl is toxic to cells and that expression of *Vc*-NorM confers resistance to this toxicity (Fig. 2A), indicating that *Vc*-NorM transports Ruboxyl. Furthermore, the micromolar affinity of Ruboxyl is equivalent to affinities reported for drug binding to *Vc*-NorM and its homologs.^{7,26} Therefore, the interaction of Ruboxyl that we have characterized here is relevant to the transport mechanism and likely not unique to this molecule. We foresee the further utilization of Ruboxyl to probe the substrate binding site(s)

on MATE transporters and the many other multidrug transporters that transport anthracyclines. $^{2,11,27-30}\,$

The EPR data indicated that the apparent binding affinity for Ruboxyl has contributions from multiple binding modes. Most interesting and informative, binding of Ruboxyl to a high affinity site on Vc-NorM is evident in the appearance of an immobilized component in the EPR lineshape and marked reduction of this component in the presence of an excess of known Vc-NorM substrates acting as competitors. This immobilized population likely represents the Ruboxyl molecules bound with higher affinity to the native substrate binding site. In contrast, non-specifically-bound Ruboxyl did not respond to the presence of competitors and had a more mobile EPR lineshape reflecting disorder of the bound molecule. We hypothesize that Ruboxyl molecules bound to Vc-NorM with high disorder are non-specifically associated with detergent molecules in complex with solubilized Vc-NorM. Given the convolution of binding modes, we report only the apparent K_D for binding of Ruboxyl to Vc-NorM in -DDM micelles. Earlier characterizations of NorM that used anisotropy as a measure for binding of doxorubicin⁷ or rhodamine 6G²⁶ in the presence of detergent have likely also reported an apparent K_D with contributions from multiple binding modes, and this convolution should be expected in all binding measurements of a hydrophobic ligand to a detergent-solubilized receptor.

In the crystal structures of Ng-NorM bound to TPP, ethidium, or rhodamine 6G, the substrates bind to the same location on the periplasmic side of the cleft between the two halves of Ng-NorM in an apparently outward-open state. We have used distances between bound Ruboxyl and seven spin-labeled sites on NorM, determined by DEER and CW-EPR spectroscopy, to triangulate the high affinity site of Ruboxyl binding using the crystal structures of Vc-NorM and Ng-NorM as a scaffold. These two structural models are very similar, but differences in helical register became apparent when choosing label positions for distance measurements. The most significant discrepancy between the structures was the position of residue 125, which sits on the top of TM 4 in Vc-NorM but is placed in the extended 3-4 loop of Ng-NorM by sequence alignment. Therefore, we compared the triangulation results from both structures in order to take advantage of the higher resolution and substrate-bound state of the Ng-NorM structure. The results of the triangulation procedure placed the position of the nitroxide of bound Ruboxyl at the edge of the periplasmic cleft near TM7. This position is consistent with the location occupied by substrates in the crystal structures of Ng-NorM and is in close proximity to the hairpin formed by TMs 7 and 8, which is proposed to move in response to ion and/or substrate binding. Because the linkage between the bulk of Ruboxyl and the nitroxide is flexible, we are unable to establish the orientation of the Ruboxyl in the binding site. Even so, the triangulated position of Ruboxyl is not consistent with occupancy of a more cytoplasmic site in the cleft as observed in the crystal structure of norfloxacin-bound Pf-MATE. 10 The data presented here indicate a single binding site and offer no evidence of ion-induced translocation of substrate between multiple sites. Indeed no effect of the coupling Na⁺ ion was observed in our experiments.

The absence of an effect of Na⁺ on Ruboxyl binding is surprising given that drug antiport by VcmA (a 99% identical ortholog of *Vc*-NorM) as well as *Vp*-NorM and *Ng*-NorM have been shown to be Na⁺-coupled.^{4,5,26} In the classical paradigm of ion-coupled antiport, transporters alternate between an inward-facing state with high affinity for substrate and low affinity for ion and an outward-facing state where the reverse is true. Mutually exclusive binding of substrate to the inward-facing state and ion to the outward-facing state induces the opposite state. The data presented here show that the location and apparent affinity of the Ruboxyl binding site is not dependent on the presence of Na⁺ under these conditions. This observation is not consistent with mutually exclusive binding of substrate and coupling ion.

One possible explanation is that we did not use a sufficient concentration of Na⁺ to elicit a structural response from NorM that would lead to substrate release. However, our preliminary observations indicate that 70 mM Na⁺ is enough to induce structural changes in NorM (Steed and Mchaourab, unpublished observations). Although mutually exclusive binding has been shown for H⁺-coupled drug antiporters, ^{31,32} no experiments have shown substrate-induced Na⁺ release or vice versa. In the only other direct study of substrate binding to a MATE transporter, Long et al.²⁶ also failed to observe a strong effect of Na⁺ on rhodamine 6G binding to Ng-NorM showing that varying Na⁺ concentration from 0 to 100 mM only shifted the K_D by 2.5 µM. The absence of a Na⁺ effect observed by these methods may indicate that the classical paradigm of antiport is an over-simplification, at least in the case of NorM. An emerging body of evidence suggests that a transport cycle, rather than proceeding by complete shifts between distinct states, involves transporters adopting multiple states in equilibrium. 33-35 Ions and substrates modulate the fractional occupancy of these states rather than shifting one to another. In this case, the effect of Na⁺ during transport may be dependent on the presence of a Na⁺ concentration gradient across the membrane such that our measurements of substrate affinity in a detergent-solubilized system at thermodynamic equilibrium may miss any effect of Na⁺. To answer the question of how Na⁺ causes substrate to dissociate will require measurements of substrate and ion binding in the presence of a gradient or measurement of trapped states in the transport cycle along with definition of how ions and substrates modulate the equilibrium among these states.

Supplementary Material

Refer to Web version on PubMed Central for supplementary material.

Acknowledgments

This work was supported by National Institutes of Health grants $F32\ GM100569$ to P.R.S. and $R01\ GM077659$ to H.S.M.

We thank Geoffrey Chang for providing the NorM expression plasmid, Hiroyasu Yamanaka for providing the BL21 7 strain, Ping Zou for assistance with the Cys-less NorM construct, and Cesar Luna-Chavez for the initiation of preliminary experiments with spin-labeled daunorubicin obtained from Natalya Rapoport. We also thank Elizabeth Nguyen for helpful discussions of Ruboxyl binding as well as Kelli Kazmier and Brandy Verhalen for critically reading the manuscript

ABBREVIATIONS

CW continuous wave

-DDM -dodecylmaltoside

DTT dithiothreitol

DEERdouble electron-electron resonance**EDDA**ethylenediamine-N, N-diacetic acid**EPR**electron paramagnetic resonance

HEPES 4-(2-hydroxyethyl)-1-piperazineethanesulfonic acid

IPTG isopropyl- -D-1-thiogalactopyranoside
 MATE multidrug and toxic compound extrusion
 MES 2-(N-morpholino)ethanesulfonic acid

Ng Neisseria gonorrhea

NTA nitrilotriacetic acid

PCR polymerase chain reaction

Pf Pyrococcus furiosus

TM transmembrane

TPP tetraphenylphosphonium

Vc Vibrio cholerae

Vp Vibrio parahaemolyticus

REFERENCES

 Higgins CF. Multiple molecular mechanisms for multidrug resistance transporters. Nature. 2007; 446:749–757. [PubMed: 17429392]

- 2. Kuroda T, Tsuchiya T. Multidrug efflux transporters in the MATE family. Biochim. Biophys. Acta. 2009; 1794:763–768. [PubMed: 19100867]
- 3. Omote H, Hiasa M, Matsumoto T, Otsuka M, Moriyama Y. The MATE proteins as fundamental transporters of metabolic and xenobiotic organic cations. Trends Pharmacol. Sci. 2006; 27:587–593. [PubMed: 16996621]
- 4. Morita Y, Kataoka A, Shiota S, Mizushima T, Tsuchiya T. NorM of vibrio parahaemolyticus is an Na(+)-driven multidrug efflux pump. J. Bacteriol. 2000; 182:6694–6697. [PubMed: 11073914]
- Huda MN, Morita Y, Kuroda T, Mizushima T, Tsuchiya T. Na+-driven multidrug efflux pump VcmA from Vibrio cholerae non-O1, a non-halophilic bacterium. FEMS Microbiol. Lett. 2001; 203:235–239. [PubMed: 11583854]
- Otsuka M, Yasuda M, Morita Y, Otsuka C, Tsuchiya T, Omote H, Moriyama Y. Identification of essential amino acid residues of the NorM Na+/multidrug antiporter in Vibrio parahaemolyticus. J. Bacteriol. 2005; 187:1552–1558. [PubMed: 15716425]
- He X, Szewczyk P, Karyakin A, Evin M, Hong W-X, Zhang Q, Chang G. Structure of a cationbound multidrug and toxic compound extrusion transporter. Nature. 2010; 467:991–994. [PubMed: 20861838]
- Vanni S, Campomanes P, Marcia M, Rothlisberger U. Ion binding and internal hydration in the multidrug resistance secondary active transporter NorM investigated by molecular dynamics simulations. Biochemistry. 2012; 51:1281–1287. [PubMed: 22295886]
- Lu M, Symersky J, Radchenko M, Koide A, Guo Y, Nie R, Koide S. Structures of a Na+-coupled, substrate-bound MATE multidrug transporter. Proc. Natl. Acad. Sci. U. S. A. 2013; 110:2099– 2104. [PubMed: 23341609]
- Tanaka Y, Hipolito CJ, Maturana AD, Ito K, Kuroda T, Higuchi T, Katoh T, Kato HE, Hattori M, Kumazaki K, Tsukazaki T, Ishitani R, Suga H, Nureki O. Structural basis for the drug extrusion mechanism by a MATE multidrug transporter. Nature. 2013; 496:247–251. [PubMed: 23535598]
- Smriti, Zou, P.; Mchaourab, HS. Mapping daunorubicin-binding sites in the ATP-binding cassette transporter MsbA using site-specific quenching by spin labels. J. Biol. Chem. 2009; 284:13904– 13913. [PubMed: 19278995]
- Omote H, Al-Shawi MK. A novel electron paramagnetic resonance approach to determine the mechanism of drug transport by P-glycoprotein. J. Biol. Chem. 2002; 277:45688–45694. [PubMed: 12244102]
- 13. Gaffney BJ, Bradshaw MD, Frausto SD, Wu F, Freed JH, Borbat P. Locating a lipid at the portal to the lipoxygenase active site. Biophys. J. 2012; 103:2134–2144. [PubMed: 23200047]
- 14. Emanuel N, Konovalova N, Povarov L, Shapiro A, Dyachkovskaya R, Suskina V, Denisova L. 13-(1-Oxyl-2, 2, 6, 6-tetramethylpiperylidenyl-4) hydrazone rubomycin hydrochloride with a paramagnetic center and a method of producing same. US Patent. 1982; 4:332–934.

 Jeschke G, Polyhach Y. Distance measurements on spin-labelled biomacromolecules by pulsed electron paramagnetic resonance. Phys. Chem. Chem. Phys. 2007; 9:1895–1910. [PubMed: 17431518]

- Borbat PP, Surendhran K, Bortolus M, Zou P, Freed JH, Mchaourab HS. Conformational motion of the ABC transporter MsbA induced by ATP hydrolysis. PLoS Biol. 2007; 5:e271. [PubMed: 17927448]
- Mchaourab HS, Steed PR, Kazmier K. Toward the Fourth Dimension of Membrane Protein Structure: Insight into Dynamics from Spin-Labeling EPR Spectroscopy. Structure. 2011; 19:1549–1561. [PubMed: 22078555]
- Yamanaka H, Kobayashi H, Takahashi E, Okamoto K. MacAB is involved in the secretion of Escherichia coli heat-stable enterotoxin II. J. Bacteriol. 2008; 190:7693–7698. [PubMed: 18805970]
- 19. Koteiche HA, Reeves MD, Mchaourab HS. Structure of the substrate binding pocket of the multidrug transporter EmrE: site-directed spin labeling of transmembrane segment 1. Biochemistry. 2003; 42:6099–6105. [PubMed: 12755611]
- 20. Pannier M, Veit S, Godt A, Jeschke G, Spiess HW. Dead-time free measurement of dipole-dipole interactions between electron spins. J. Magn. Reson. 2000; 142:331–340. [PubMed: 10648151]
- 21. Jeschke G, Chechik V, Ionita P. DeerAnalysis2006—a comprehensive software package for analyzing pulsed ELDOR data. Appl. Magn. Reson. 2006; 498:473–498.
- 22. Chiang YW, Borbat PP, Freed JH. The determination of pair distance distributions by pulsed ESR using Tikhonov regularization. J. Magn. Reson. 2005; 172:279–295. [PubMed: 15649755]
- Zou P, Mchaourab HS. Alternating Access of the Putative Substrate-Binding Chamber in the ABC Transporter MsbA. J. Mol. Biol. 2009; 393:574–585. [PubMed: 19715704]
- 24. Le Maire M, Champeil P, Moller JV. Interaction of membrane proteins and lipids with solubilizing detergents. Biochim. Biophys. Acta. 2000; 1508:86–111. [PubMed: 11090820]
- 25. Polyhach Y, Bordignon E, Jeschke G. Rotamer libraries of spin labelled cysteines for protein studies. Phys. Chem. Chem. Phys. 2011; 13:2356–2366. [PubMed: 21116569]
- 26. Long F, Rouquette-Loughlin C, Shafer WM, Yu EW. Functional cloning and characterization of the multidrug efflux pumps NorM from Neisseria gonorrhoeae and YdhE from Escherichia coli. Antimicrob. Agents Chemother. 2008; 52:3052–3060. [PubMed: 18591276]
- 27. Edgar R, Bibi E. MdfA, an Escherichia coli multidrug resistance protein with an extraordinarily broad spectrum of drug recognition. J. Bacteriol. 1997; 179:2274–2280. [PubMed: 9079913]
- 28. Bolhuis H, Poelarends G, Van Veen HW, Poolman B, Driessen AJ, Konings WN. The Lactococcal lmrP gene encodes a proton motive force-dependent drug transporter. J. Biol. Chem. 1995; 270:26092–26098. [PubMed: 7592810]
- 29. Gottesman MM, Pastan I. Biochemistry of multidrug resistance mediated by the multidrug transporter. Annu. Rev. Biochem. 1993; 62:385–427. [PubMed: 8102521]
- 30. Eicher T, Cha H, Seeger M. a, Brandstätter L, El-Delik J, Bohnert J. a, Kern WV, Verrey F, Grütter MG, Diederichs K, Pos KM. Transport of drugs by the multidrug transporter AcrB involves an access and a deep binding pocket that are separated by a switch-loop. Proc. Natl. Acad. Sci. U. S. A. 2012; 109:5687–5692. [PubMed: 22451937]
- Soskine M, Adam Y, Schuldiner S. Direct evidence for substrate-induced proton release in detergent-solubilized EmrE, a multidrug transporter. J. Biol. Chem. 2004; 279:9951–9955. [PubMed: 14701800]
- 32. Fluman N, Ryan CM, Whitelegge JP, Bibi E. Dissection of mechanistic principles of a secondary multidrug efflux protein. Mol. Cell. 2012; 47:777–787. [PubMed: 22841484]
- 33. Claxton DP, Quick M, Shi L, De Carvalho FD, Weinstein H, Javitch JA, Mchaourab HS. Ion/substrate-dependent conformational dynamics of a bacterial homolog of neurotransmitter:sodium symporters. Nat. Struct. Mol. Biol. 2010; 17:822–829. [PubMed: 20562855]
- 34. Hänelt I, Wunnicke D, Bordignon E, Steinhoff H-J, Slotboom DJ. Conformational heterogeneity of the aspartate transporter Glt(Ph). Nat. Struct. Mol. Biol. 2013; 20:210–214. [PubMed: 23334291]
- 35. Georgieva ER, Borbat PP, Ginter C, Freed JH, Boudker O. Conformational ensemble of the sodium-coupled aspartate transporter. Nat. Struct. Mol. Biol. 2013; 20:215–221. [PubMed: 23334289]

$$H_3C$$
 H_3C
 H_3C

Figure 1. Structure of Ruboxyl.

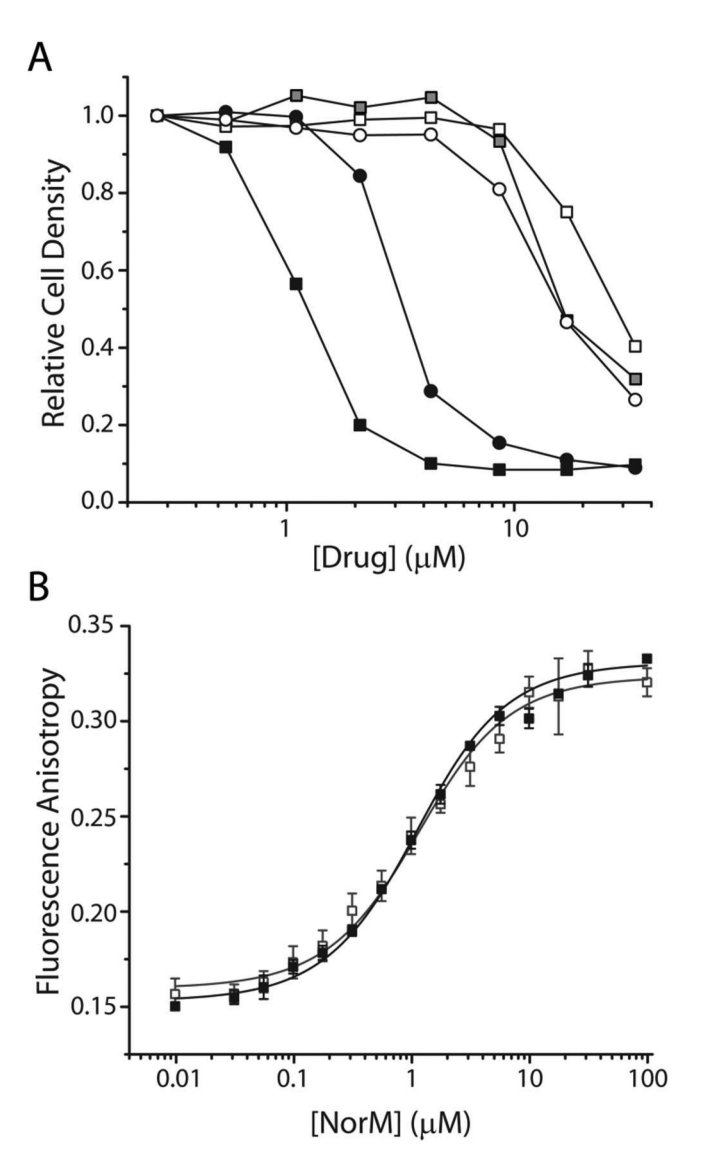


Figure 2. Ruboxyl is a substrate of NorM

A) Ruboxyl resistance of drug-sensitive BL21 7 cells was measured using a growth complementation assay. Cells expressing WT NorM (white), Cys-less NorM (gray), or harboring empty pET19b (black) were cultured in 50% LB containing 0.1 mg/ml ampicillin, 10 μ M IPTG to induce NorM expression, and 0-34 μ M Ruboxyl (circles) or doxorubicin (squares). Optical density of the cultures relative to the culture with the lowest drug concentration is plotted. B) *In vitro* binding of Ruboxyl by wild type (black) or Cys-less (white) NorM was measured by fluorescence anisotropy. Anisotropy values were collected for 25 μ l samples containing 0.2 μ M Ruboxyl and 0.01-100 μ M NorM in GF buffer. The solid lines are non-linear, least-squares fits assuming a single binding site with an apparent K_D of 0.9 μ M (WT) or 1 μ M (Cys-less).

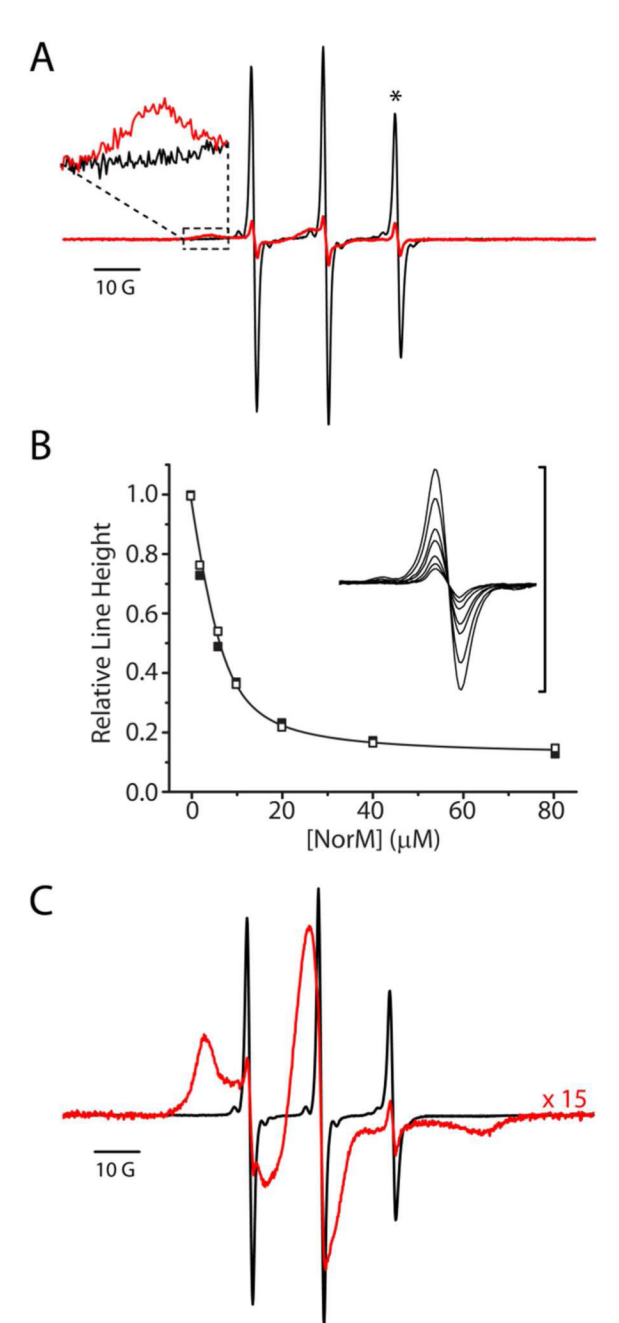


Figure 3. Immobilization of bound Ruboxyl

CW-EPR spectra were collected for 25 μ l samples containing 7 μ M Ruboxyl and 0-80 μ M NorM in GF buffer. A) The spectrum of free Ruboxyl (black) shows sharp lines characteristic of a mobile nitroxide. The high field resonance line is marked with a star (*). The spectrum of Ruboxyl with 80 μ M NorM (red) shows features of an immobilized nitroxide and diminished intensity of sharp resonance lines. The inset shows the broadened low-field line. B) Relative height of the high field resonance line (inset) decreases with increasing NorM concentrations. Line heights were normalized to that of free Ruboxyl. Similar binding was observed in the presence (closed squares) or absence (open squares) of 20 mM NaCl. A non-linear, least-squares fit of the Na⁺-free condition assuming a single binding site with an apparent K_D of 1.8 μ M (solid line) fits well with both binding curves.

The fit of the Na⁺ condition (not shown) is superimposable, and has an apparent K_D of 1.5 μ M. C) The spectrum of 80 μ M free Ruboxyl (black) compared to the spectrum of 80 μ M Ruboxyl in the presence of 440 μ M NorM (red). The bound spectrum was multiplied by 15 to show the details of the lineshape.

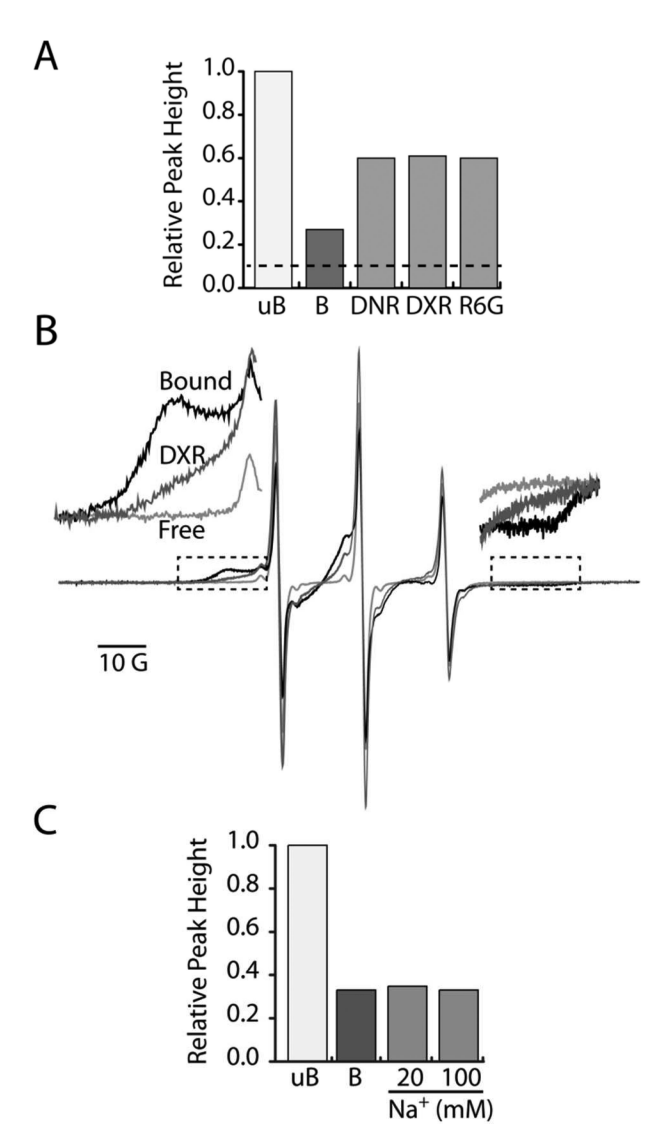


Figure 4. Competition for the substrate binding site

A) Peak height of the high field resonance line of 7 μ M Ruboxyl in GF buffer with 20 mM NaCl (uB) is compared to peak heights of Ruboxyl bound to 10 μ M NorM without competitor (B) or in the presence of 350 μ M daunorubicin (DNR), doxorubicin (DXR), or rhodamine 6G (R6G). Peak heights were normalized to that of free Ruboxyl. The dashed line indicates the fraction of the signal resulting from detergent-bound Ruboxyl. B) CW-EPR spectra of bound Ruboxyl (110 μ M NorM; 80 μ M Ruboxyl) in the presence (dark gray) or absence (black) of 2.8 mM doxorubicin. The spectrum of 80 μ M Ruboxyl without NorM is plotted (30% of full signal) in light gray for lineshape comparison. Inset spectral details show the disappearance of the immobilized component in the presence of doxorubicin. C) Peak height of the high field resonance line of 7 μ M Ruboxyl in GF buffer (uB) is compared to peak heights of Ruboxyl bound to 10 μ M NorM without Na⁺ (B) or in the presence of 20 or 100 mM NaCl.

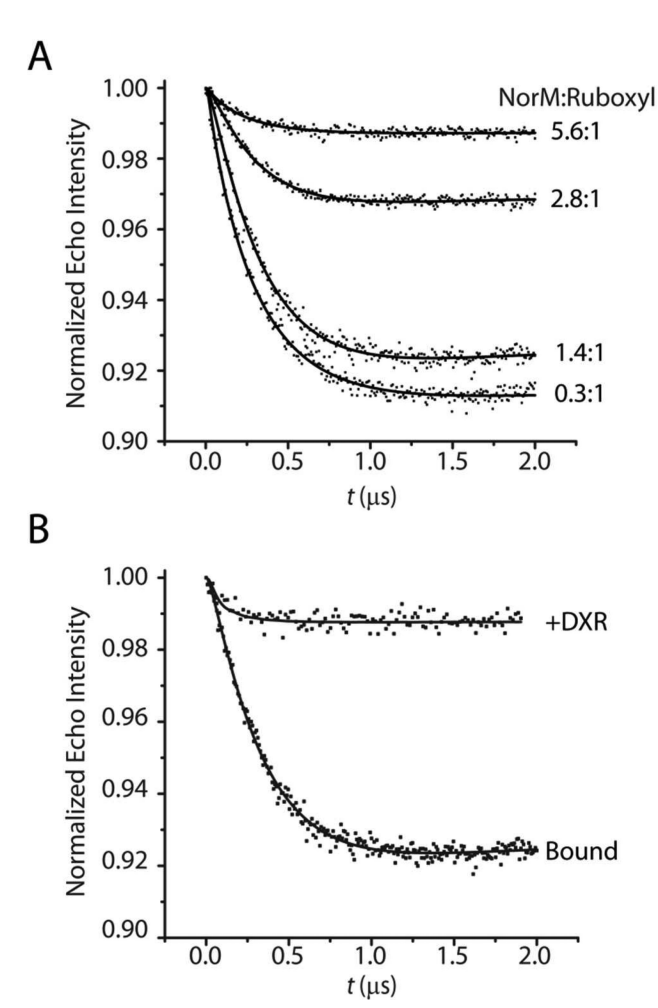


Figure 5. Binding of additional Ruboxyl molecule(s) is non-specific A) DEER decays are shown for samples containing 80 μ M Ruboxyl and 20 – 440 μ M NorM (the molar ratio of NorM to Ruboxyl is noted) in GF buffer with 20 mM NaCl. B) DEER decays are shown for bound Ruboxyl (110 μ M NorM; 80 μ M Ruboxyl) in the absence or presence of 2.8 mM doxorubicin.

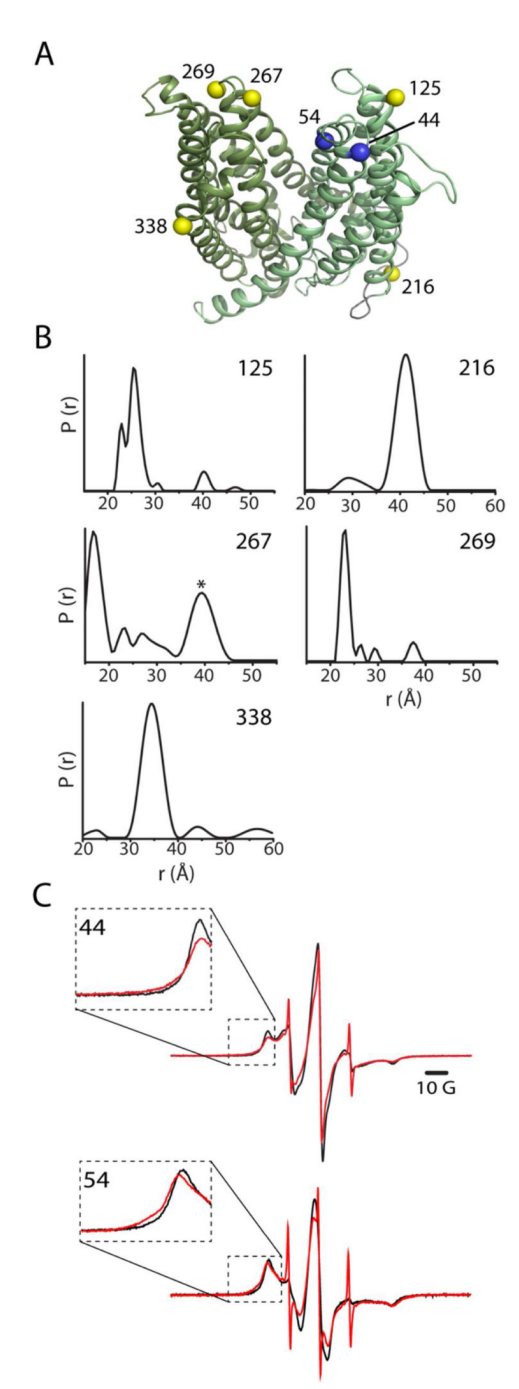


Figure 6. Distance measurements to bound Ruboxyl

A) The positions of spin labels used for distance measurements with DEER (yellow) or CW-EPR (blue) are shown as spheres on the structure of *Vc*-NorM (PDB: 3MKT). B) Distributions of distances (r) between Ruboxyl and spin labels at positions 125, 216, 267, 269, and 338. Samples were prepared with NorM and Ruboxyl maintaining a NorM:Ruboxyl molar ratio of 3.75:1. The peak marked with * in the distance distribution from position 267 arose from aggregation, which was evident in the DEER decay as a long, poorly defined component (Fig. S2). C) CW-EPR spectra in the presence (red) or absence (black) of Ruboxyl are shown for labels at positions 44 and 54. Spectral details show broadening of the low-field resonance line.

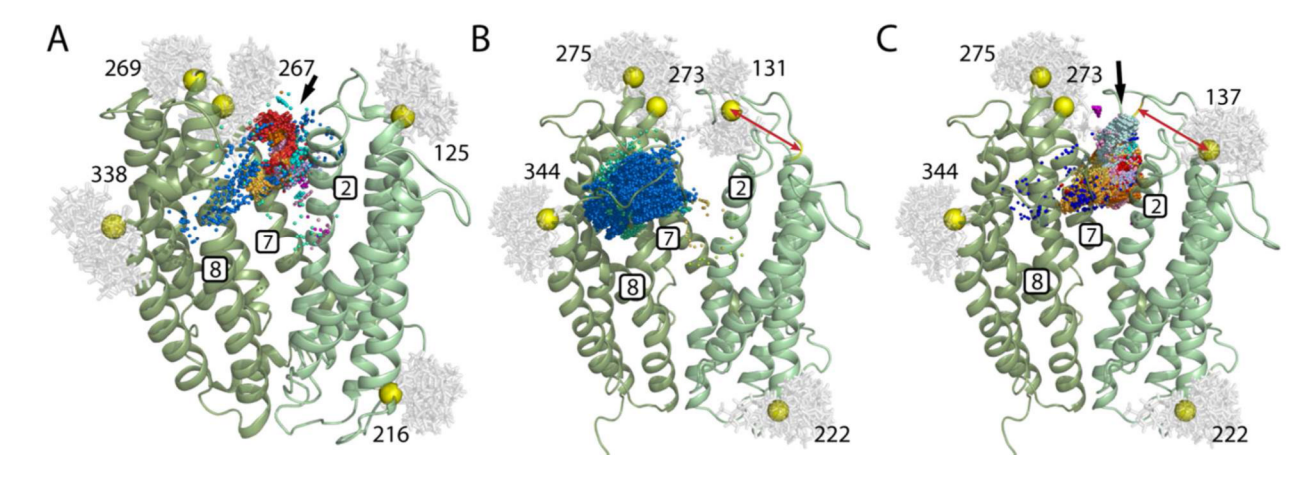


Figure 7. Location of bound Ruboxyl

Ribbon representations of the crystal structures of *Vc*-NorM (A) and *Ng*-NorM (B and C) are shown from a periplasmic perspective. TM 1 has been omitted for clarity. Positions of spin labels are shown as yellow spheres denoting the C position surrounded by the cloud of most likely rotamers of the spin label side chain generated by MMM. Possible positions of the Ruboxyl nitroxide are shown as small spheres, where coloring differentiates positions derived from triangulation using different sets of three distances. A) Using the crystal structure of *Vc*-NorM as a scaffold resulted in a band of potential Ruboxyl nitroxide positions on the periplasmic side of the cleft with a confluence of points (arrow) lying between TMs 2 and 7. B) Using the crystal structure of *Ng*-NorM and the 3-4 loop position of *Vc*-NorM 125 (*Ng*-NorM 131) results in nitroxide positions surrounding TM 8. Combinations of distances that do not include position 125 are omitted. C) Using the crystal structure of *Ng*-NorM and the TM 4 position of *Vc*-NorM 125 (*Ng*-NorM 137) results in a confluence of potential Ruboxyl nitroxide positions (arrow) similar to that seen with *Vc*-NorM (Panel A). The red arrow in panels B and C indicates the difference between the placement of the sequence equivalent or the structural equivalent of *Vc*-NorM residue 125.

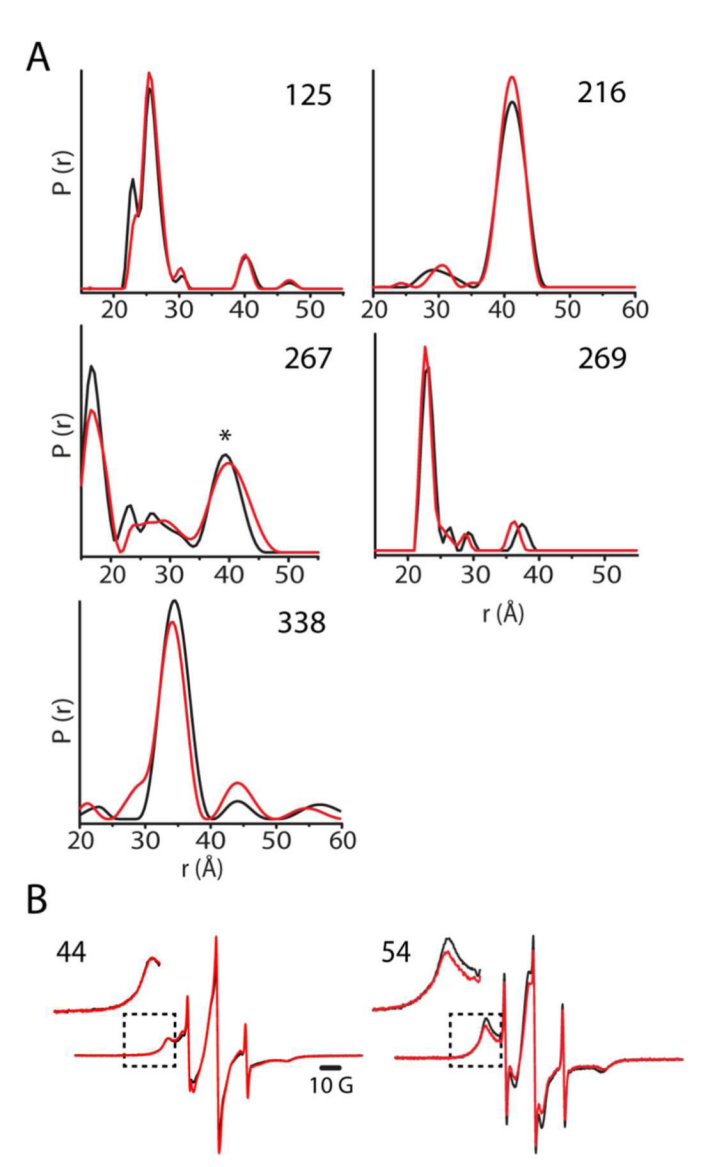


Figure 8. Effect of Na⁺ on measured distances to bound Ruboxyl

A) Distributions of distances (r) between Ruboxyl and spin labels at positions 125, 216, 267, 269, and 338. Samples were prepared in the presence (red) or absence (black) of 70 mM NaCl with NorM and Ruboxyl maintaining a NorM:Ruboxyl molar ratio of 3.75:1. B) CW-EPR spectra of Ruboxyl bound to NorM spin-labeled at position 44 or 54 in the presence (red) or absence (black) or 70 mM NaCl. Spectral details show the low-field resonance line. The peak marked with * in the distance distribution from position 267 arose from aggregation, which was evident in the DEER decay as a long, poorly defined component (Fig. S2).

Table 1Binding Affinities of Wild Type and Cys-less NorM

	Apparent K _D ^a		
NorM	Doxorubicin	Daunorubicin	Ruboxyl
		μM	
Wild type	0.6	n.d. b	0.9
Cys-less	0.6	2.5	1.0

 $^{^{\}textit{a}} \text{Calculated from a non-linear, least-squares fit of fluorescence anisotropy data (see "Experimental Procedures")}$

b n.d., not determined